

CHAPTER 11

ELECTRICAL PROPERTIES

Electrical properties of CuInS_2 films

Electronic structure of group I-III-VI₂ compounds are ternary analogs of II-VI Zincblende compounds. While, the energy band structure of ternary differs from that of binary compound. The valence bands of most binary are composed of S-and P-like orbitals, whereas , the upper most valence bands of a ternary compound are profoundly influenced by the proximity of noble-metal d-levels. This leads to several anomalous features of the energy band.

The direct energy gap observed in the group I-III-VI₂ compounds are low relative to the energy gap in the II-VI analogs by amount up to 1.6 ev. Also, the spin-orbit splitting of the upper most valence band are reduced relative to binary analogs, due to a partial cancellation of the positive spin-orbit parameters for p-levels and the negative spin-orbit parameters for d-levels.

Several ternary compounds can be obtained in p-and n-type . In addition, some of them can be made p-type and have direct energy gap in the visible and ultraviolet regions. The p-type conductivity observed in Cu I-III-VI₂ compounds is surprising . Since, the binary analogs II-VI sulfides and selenides cannot be made usefully p-type . While, the intrinsic defects are playing a major role in determining the conductivity. Also, there is a moderately sharp energy boundary between those Cu-compounds which can be made both p-and n-type and those which are only p-type.

CuInS_2 with a direct gap of 1.5 eV has been made p-and n-type by annealing under maximum or minimum sulfur pressure. The native defects may be active and share with large fraction in the conduction mechanism due to the non-stoichiometric composition which is favorably recommended in chalcopyrite compounds.

It is expected that Cu-does not participate in the covalent bonding to any great extent. That is, most of the covalent nature of the bonding is due to the group - III- and - VI-atoms. Therefore, the energy of formation of Cu-vacancy acceptors should be smaller . If there exist some Cu-interstitial which act as donors, then, the Cu-vacancies will compensate them and the system yield a high resistance values. This phenomena depend on the experimental values of resistance. Two opposite ideas have been presented to identify the activation energy in the low temperature region. A value of 0.27 eV has been appointed out to the donor level produced by the excess Cu-interstitials or an acceptor level due to Cu-vacancy . As a matter of fact, Tell and Kasper (137) found an activation energy of 0.5 eV in CuGaS_2 which was attributed to Cu-vacancy.

5.A. D.c. Measurement

5.A.1. Chemically deposited films

Electrical properties of chemically deposited CuInS_2 films of different thickness and annealing at different temperatures were studied. At first, the as-deposited films was taken for measurements after electrodes were done by silver paste. The variation of resistance with increasing the temperature from room temperature up to 573 K , the film thickness is varied from 150 nm to 300 nm, Figure (5.1), shows the variation of , R

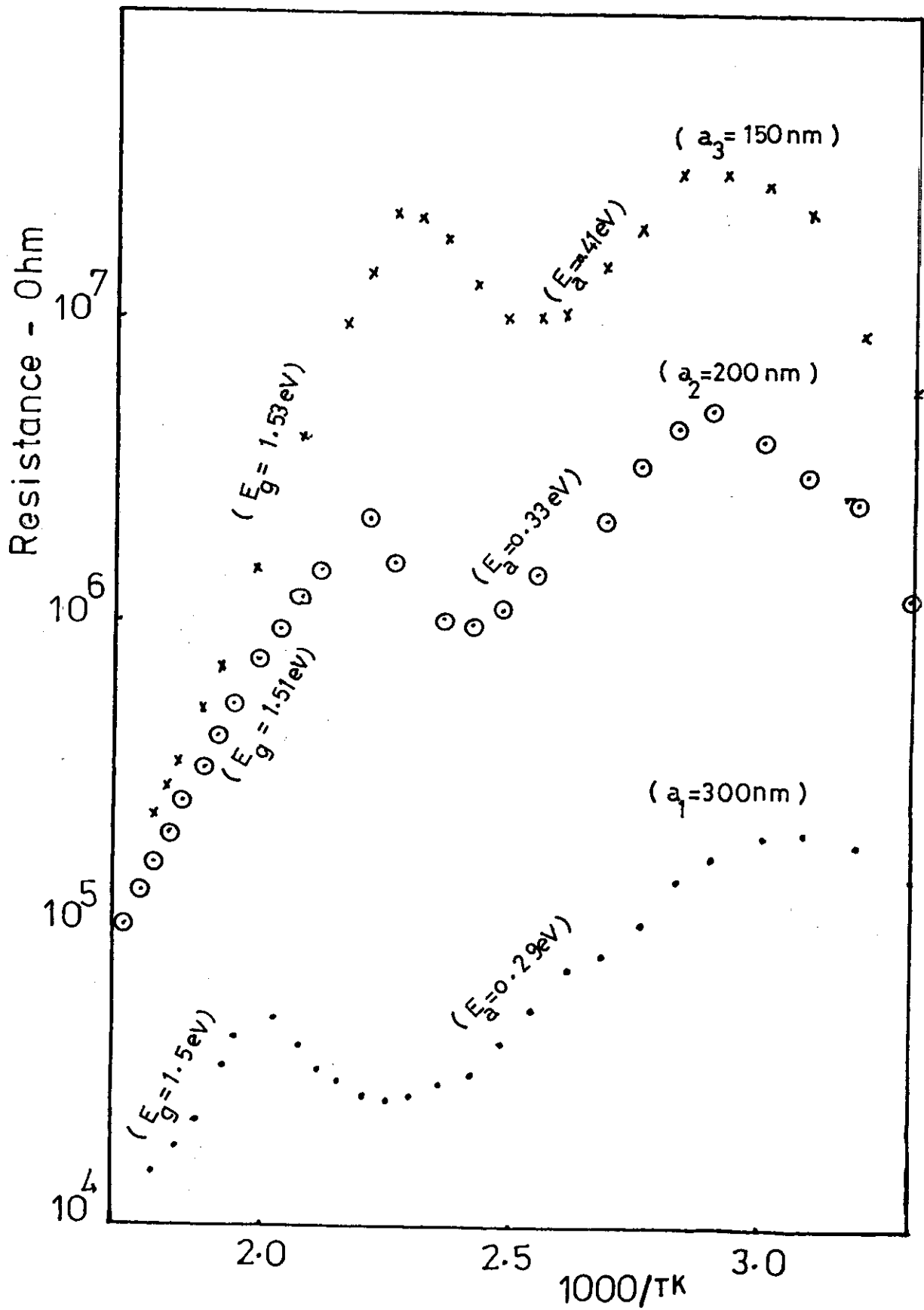


Figure (5 . 1)

versus $1/T$ for different thicknesses [under the same condition of the deposited layers]. It can be noticed that, the resistance of the as-deposited films show a low values at room temperature. The first heating run of measurement carried on the as-deposited films show a non-stable curve of (R versus $1/T$) at low temperature < 400 K . This anomaly in the behaviour of R vs. $1/T$ was noticed by other workers (133,113). It was attributed that at temperature below 373 K, chemical diffusion of copper can change the composition of CuInS_2 and its electrical conductivity. It is well known that in case of chemical deposition of CuInS_2 , free ions of Cu, In, S are released from their complexes. Later on, Cu_2S , In_2S_3 are formed, at low temperature some excess of cation still a part of reaction. Accordingly, the deposits may contain free ions of cation and anion still unreacted, intermediate phases of Cu_2S , In_2S_3 and a single phase of CuInS_2 . As the matter of fact the free cations and anions when diffused may act as doners in case of cation and acceptor in case of anions. We believe that the activation energy Table (5.1), $E_a = (0.29 - 0.41 \text{ eV})$ in the low temperature range [300 K - 503 K] corresponding to a deep donor level due to the cations of Cu. At higher temperature $T > 400$ K a pocket of resistivity was shown which is shifted to the higher temperature side with increasing the film thickness. The origin of this pocket is due to precipitation of a more conductive secondary phases, such as traces of Cu and In . As increasing temperature > 500 K the curve of , R versus $1/T$ was stable and decreases linearly with increasing temperature. The slope of this region gave an (energy gap) compatible with the energy gap (E_g) of CuInS_2 (1.5-1.53eV) Table (5.1). The value of E_g decreasing linearly with increasing the film thickness due to the reduction of the grain boundary potential.

TABLE (5.1)

Film thickness (nm)	Low region		High region	
	TK	activation energy (eV)	TK	energy gap (eV)
$a_1 = 300$	300 - 503	0.29	500 - 600	1.5
$a_2 = 200$	300 - 453	0.33	453 - 600	1.51
$a_3 = 150$	300 - 433	0.41	433 - 600	1.53

As the film consists of grains or islands separated by deposits free regions. For the current to pass through, the charge carriers have to be transferred from one island to the nearest one either through the vacuum between the islands or through the substrate. The mechanism of carriers transfer is then affects to some extent the resistivity of the film through the charge carriers mobility. It was noticed that this mechanism is temperature dependent i.e. the mechanism is an activated process. The thermionic emission of charge carriers across the island intergaps had been proposed as a possible conduction mechanism (139). Accordingly, the current depends exponentially on the height of potential barrier which itself depends on the interdistance between the islands or grains. Later on, the work in this field revealed a measurable current at very low temperature at which the thermionic emission may be ignored. These views suggests another mechanism which is the tunneling of the charge carries across the interisland gaps. The tunnelling current was found to be more sensitive to the intergaps

than the thermionic current. The energy which is electrostatic in nature, where "e" is the electronic charge and "r" is the island or grain size. If one consider two islands of dimension "r" and separated by a distance "R", at any temperature the number of carriers is given by

$$n \propto N e^{-\epsilon / KT} \quad (5.1)$$

where

ϵ is $\sim e^2 / r$ and N is the total number of islands in the film. In this case there should be an activation energy whatever its value which should be added to any other energy activated the transport mechanism. If we assume that the number of carriers jump to the top of the Fermi-surface is thermally activated and given by :

$$n \propto N e^{-\Delta E_a / KT} \quad (5.2)$$

then the number of charge carriers taken part in the transport mechanism is

$$n \propto n_1 e^{-\frac{e^2 / r}{KT}} \quad (5.3)$$

this leads finally to;

$$n \propto e^{-\Delta E_a / KT} e^{-\epsilon / KT}$$

i.e.

$$n \propto e^{-(\Delta E_a + \epsilon) / KT} \propto e^{-E_g / 2 KT} \quad (5.4)$$

where $\Delta E_g = 2 (\Delta E_a + \epsilon)$ is the energy gap. i.e. the number of the charge carriers is controlled by at least two thermally activated process, the first is the band-band transition and the second is the tunnelling at grain boundary

between the different grains. This conclusion should depend on the conductivity which must be then affected by grain size which itself depends on the film thickness; i.e. as the film goes thin the island interdistance increases and the tunneling activation energy increases as well then the activation energy for the transport mechanism increases as well.

The first heating run for all samples was cooled at room temperature again and ρ , R versus $1/T$ is shown in figure (5.2). It can be noticed that, the curve is irreversible, figure (5.1,5.2). In general, as the temperature decreases ρ , R increases in two linear relations. The first, or low temperature region with activation energy varied between (0.1-0.25 eV). The second, or higher temperature region with energy gap, varied between (1.5-1.53 eV), this values are compatible with the energy gap of CuInS_2 Table (5.2). From this figure (5.2), it can be noticed that, the pocket of resistivity is revealed. This effect is due to an equilibrium redistribution and relaxation of atoms within the basic chalcopyrite of CuInS_2 when heated up to 500k.

TABLE (5.2)

Film thickness (nm)	Low region		High region	
	TK	activation energy (eV)	TK	energy gap (eV)
$b_1 = 300$	300 - 423	0.1	423 - 600	1.5
$b_2 = 200$	300 - 393	0.198	493 - 600	1.51
$b_3 = 150$	300 - 373	0.248	373 - 600	1.53

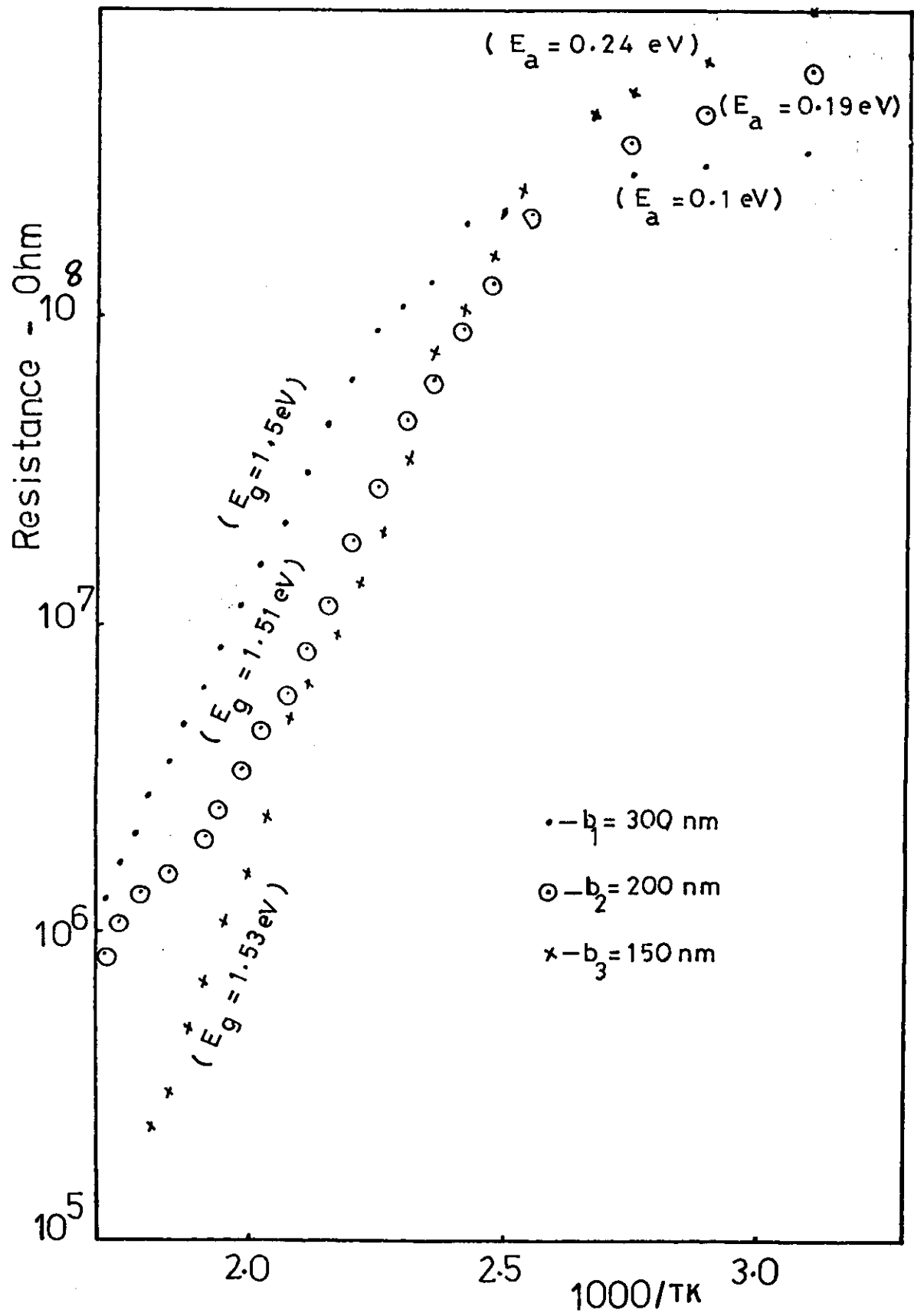


Figure (5 . 2)

The effect of heat-treatments of chemically deposited CuInS_2 films were also studied. Films of the same thickness (~ 150 nm) was heat-treated at different temperatures before electrical measurements. Figure (5.3) shows (ρ versus $1/T$) for these films heated up to : a) 373 K, b) 473 K, c) 573 K and d) 673 K in sulfur gas pressure. It can be noticed that, heating the film up to 373 K still unstable in the low temperature region curve (a) i.e. this temperature 373 K not enough to complete the reaction and produce a single phase of CuInS_2 . The second region > 400 K, the curve is stable and give a linear relation with ρ , energy gap ~ 1.55 eV. While the film heated up to 473 K, 573 K and 673 K before electrical measurements is shown in curves (b,c,d). It can be noticed that, at room temperature, resistance is changed from low to high values. As the temperature increases, ρ versus $1/T$ decreases linearly with stable value. The low temperature region gave an activation energy ($E_a \sim .25 - 0.4$ eV), which is due to the presence of deep donor level due to Cu,In interstitial or S vacancies. The high temperature region yield a value of (1.5-1.55 eV) which is compatible with the energy gap of CuInS_2 [Table 5.3] .

TABLE (5.3)

Annealing temperature T K	Low region		High region	
	TK	activation energy (eV)	TK	energy gap (eV)
a - 373	300 - 393	0.26	393 - 600	1.55
b - 473	300 - 373	0.29	373 - 600	1.53
c - 573	300 - 353	0.33	353 - 600	1.52
d - 673	300 - 333	0.39	333 - 600	1.5

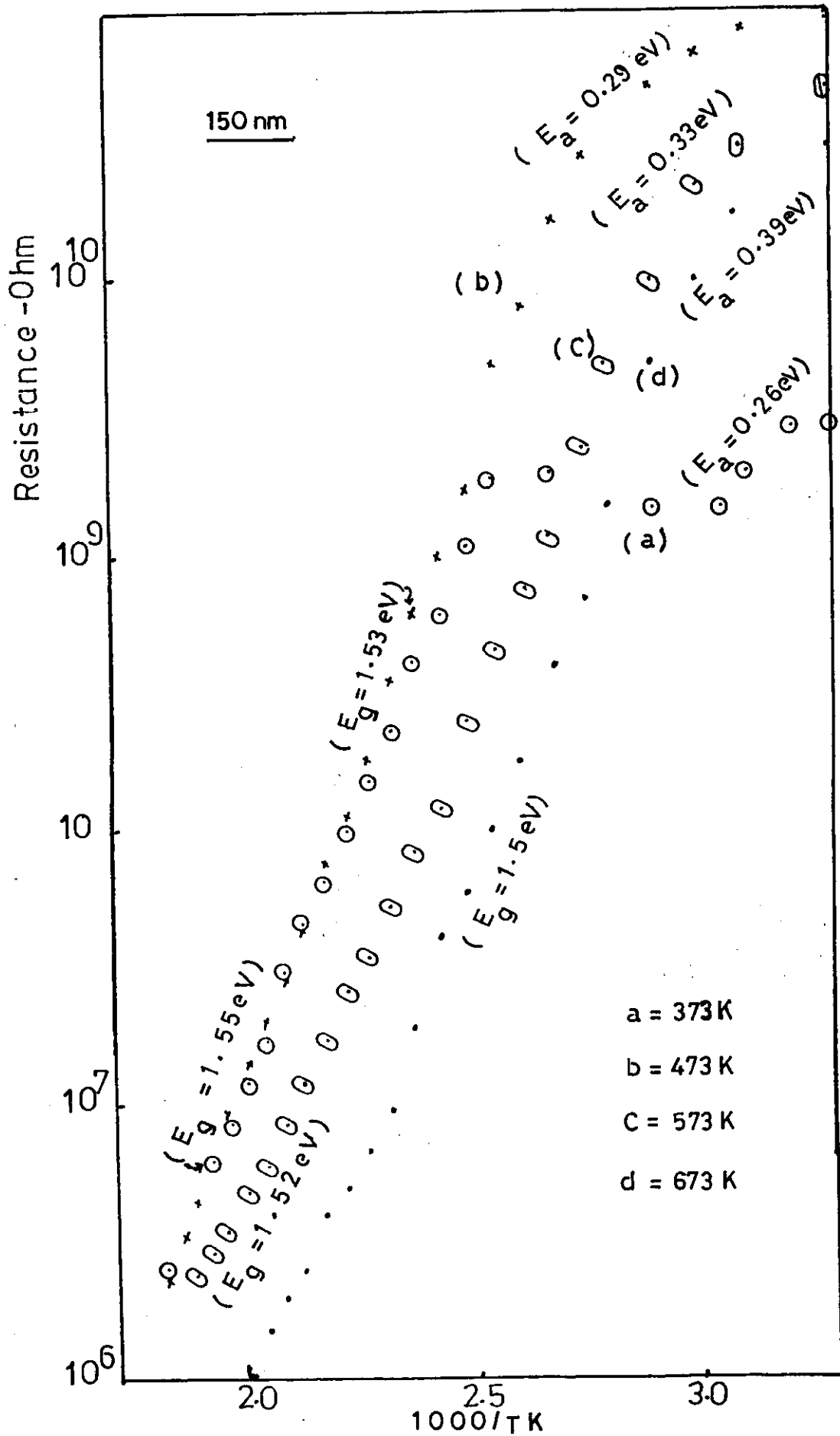


Figure (5.3)

In general, behind the clean of the film from extra phases and changing the resistance from low to high by heat-treatment, the energy gaps measured was decreased as the temperature of annealing increases [Figure (5.4), Table (5.3)]. This decrease in, E_g , results from motional narrowing due to diffusion of the spin-carrying copper ions. These results agree with other authors⁽¹¹¹⁾, and according to this equation :

$$E_g = E_g(0) - aT^2 / (T + \theta) \quad (5.5)$$

where $E_g(0)$ is the energy gap at, 0°K ; a , is an empirical constant, and θ is approximately the 0°K Debye temperature. The decrease in R was noticed in figure (5.5) for film annealed in sulfure gas pressure relative to the annealed without sulfure. it was attributed to addition of excess holes due to sulfure which increase the number of carriers, later in, a decrease in resistance.

5.A.2 . D.C.results of thermally evaporated films

Electrical resistivity of CuInS_2 films prepared by thermal evaporation were studied by d.c. measurements. At first, films with different thickness were prepared from the single phase CuInS_2 powder. After electrodes were made from silver paste which show ohmic contact, the as-deposited films was taken for d.c electrical measurements. Figure (5.6) shows the first run of heating for the different film thicknesses (R versus $1/T$). At room temperature, films show very high resistances as well known the Cu-compounds readily made p-type (sulfur saturated) (42,98).

As the temperature increases, the resistance decreases slowly at low temperature range, up to 400 K. The activation energy calculated with this region $E_a \sim 0.08 - 0.2 \text{ eV}$ [Table (5.4)] which is the order of the ionization

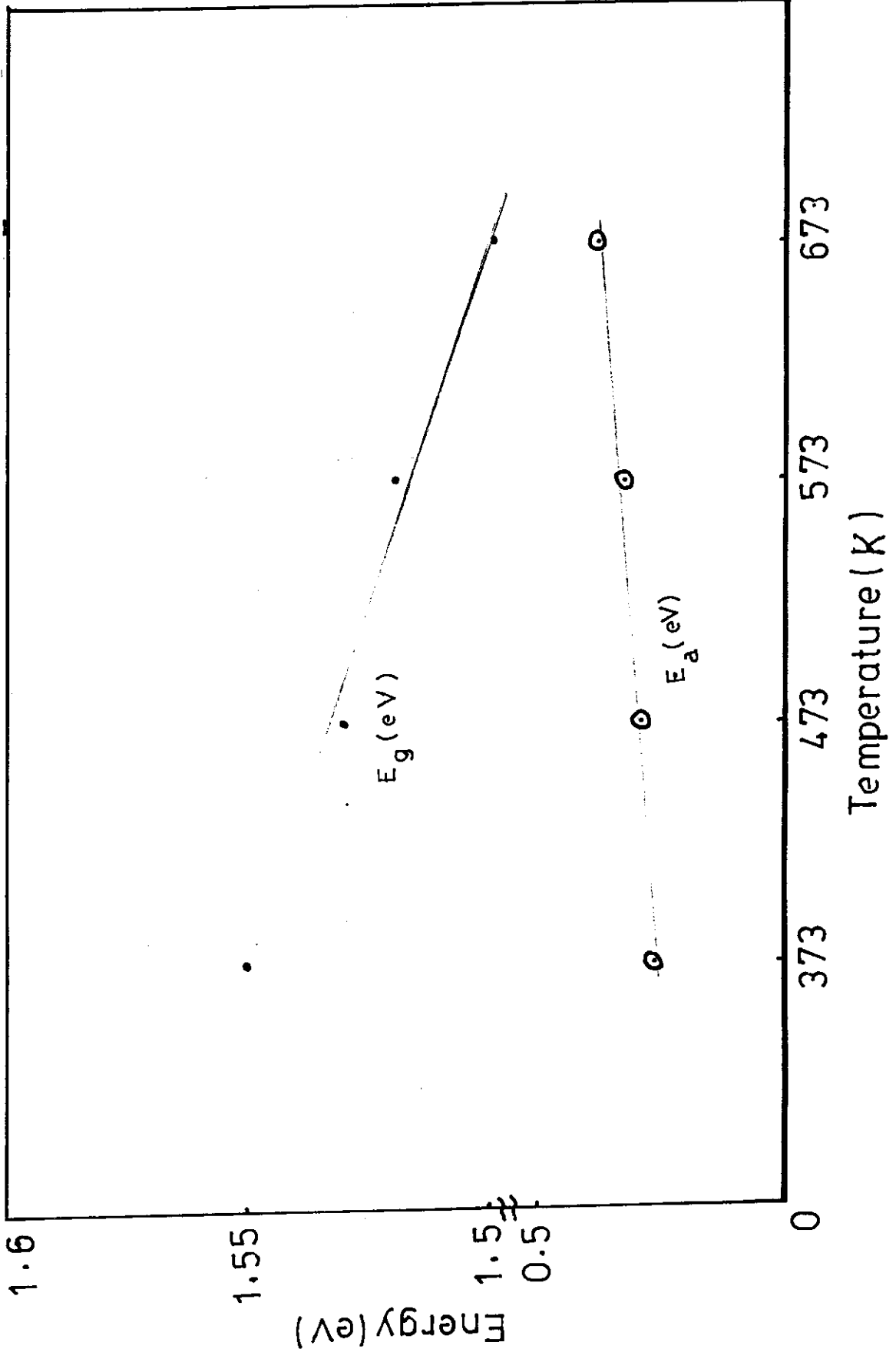


Figure (5. 4)

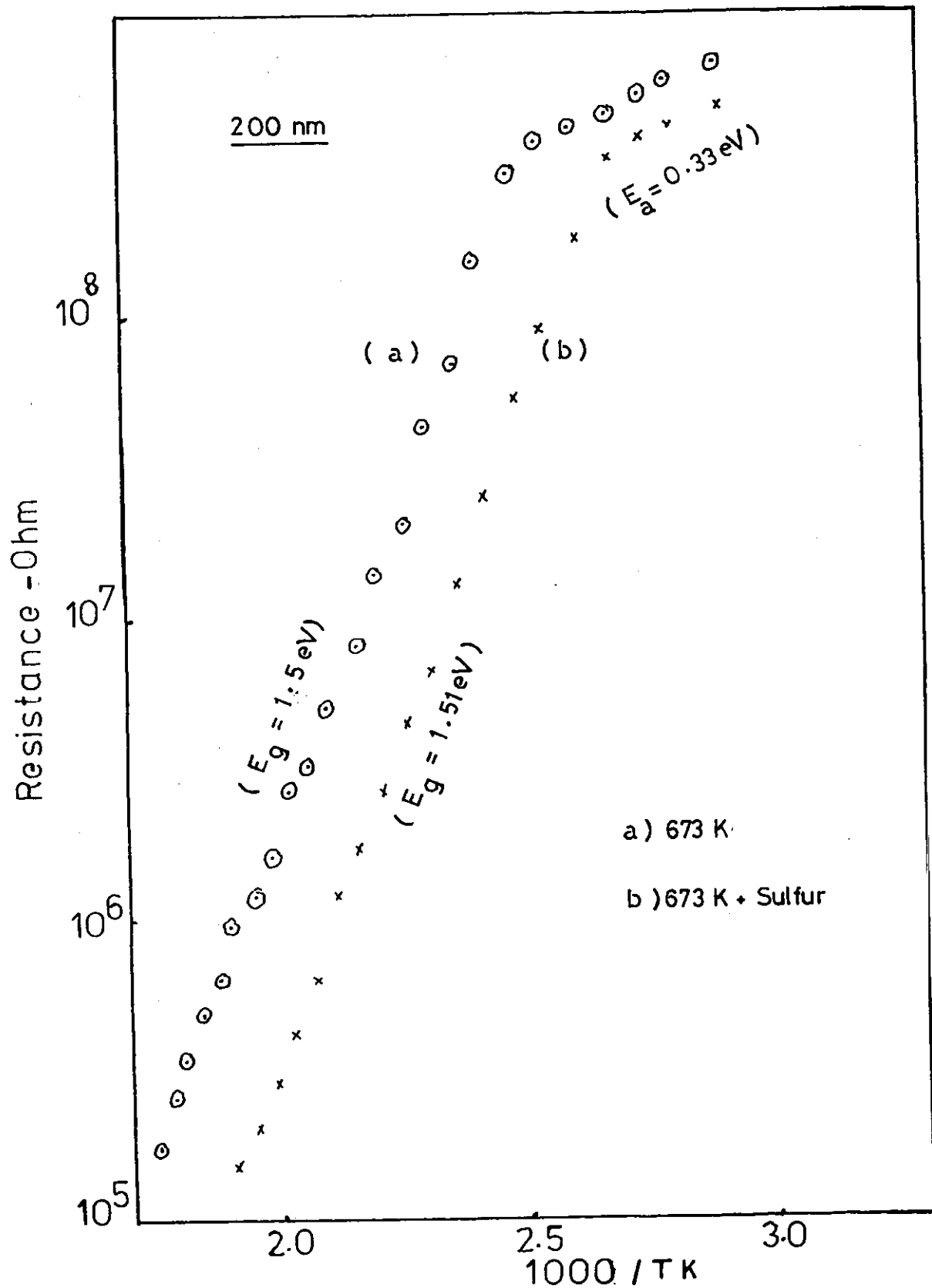


Figure (5.5)

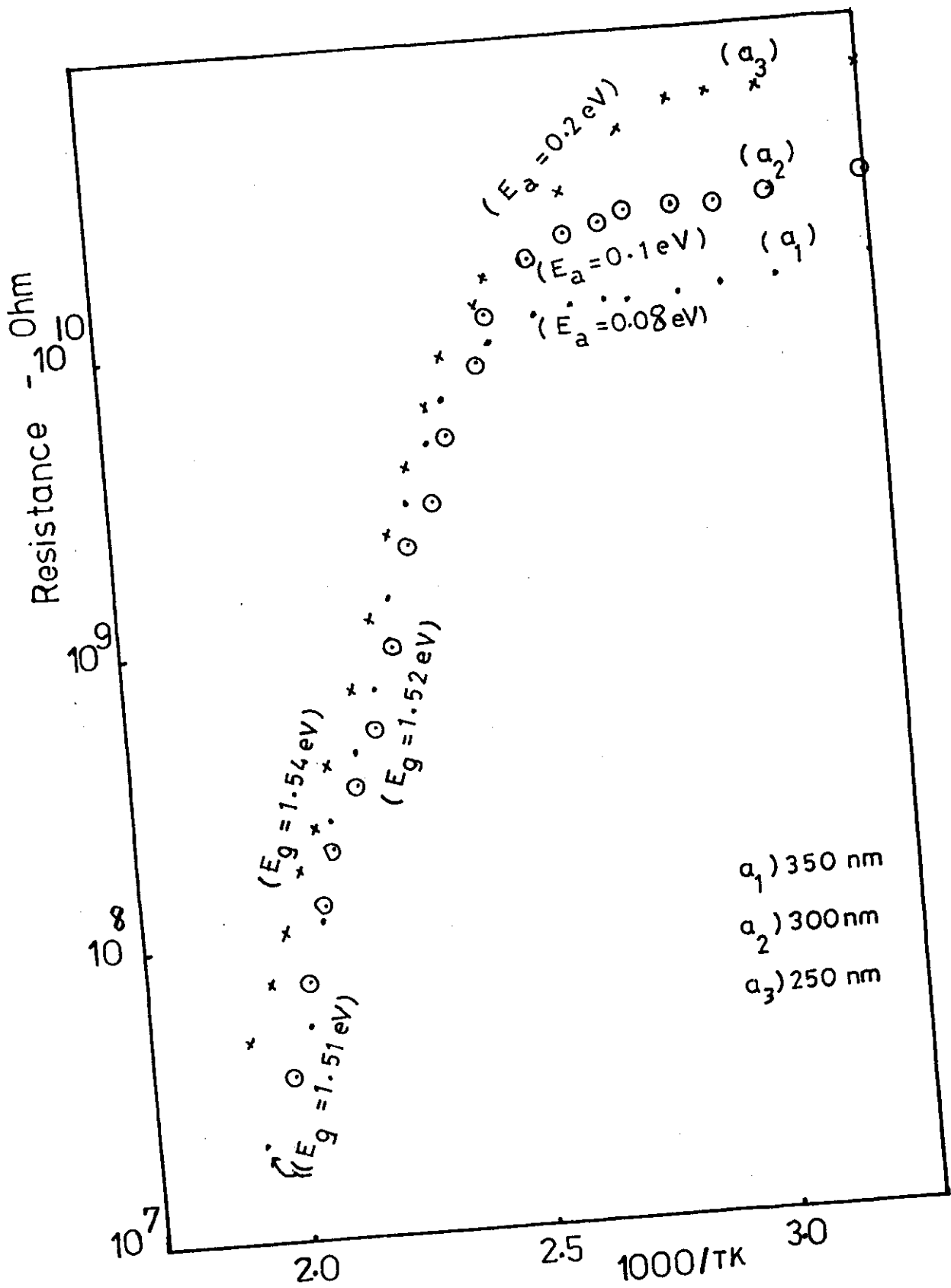


Figure (5.6)

$a_3 - 250$	300 - 353	0.2	353 - 600	1.54
-------------	-----------	-----	-----------	------

energy of the native defects. It was noticed that the resistance is temperature independent up to about 400 K. Which means that to great extent the charge carriers mobility is not controlled by thermal vibration scattering but the lattice defect is too large and mainly control the charge carriers migration in this range of temperature. Besides, in this lower range of temperature the conductivity is mainly extrinsic, while above 400 K it starts to be intrinsic, in the high temperature region the resistance decreased exponentially with temperature. The energy gap just corresponding to the energy gap 1.5-1.54 eV, [Table 5.4], which is compatible with the energy gap of CuInS₂.

In general, the activation energies change with thickness i.e. as the thickness increases, E_g decreases as mentioned in section (5.A). Also, as the thickness increases the temperature range of extrinsic increases which attributed to the number of native defect or extrinsic carriers increase. Moreover, the range separate the extrinsic region and intrinsic region called the depletion range. Also, the temperature of this range called the depletion

temperature . Below this temperature, the conductivity depends on the concentration of impurity in the specific semiconductor and the forbidden band width for fixed impurity concentration. Where after this temperature the conductivity depends on the intrinsic (band-band transition) of the semiconductor. This transition temperature as may easily be seen will be determined by the equation (140) :

$$T_{\text{dep}} = \frac{\Delta E_0}{k \ln \frac{N_c(T_{\text{dep}}) N_v(T_{\text{dep}})}{2N_d^2}} \quad (5.6)$$

i.e. if the transition from impurity to intrinsic conductivity is defined by the condition

$$P = N_d \quad \text{or} \quad n = 2N_d$$

The transition temperature as may be seen

$$Pn = n_i^2 = 2N_d^2 = N_c N_v e^{\frac{-\Delta E_0}{K(T_{\text{dep}})}} \quad (5.7)$$

For a fixed N_d the temperature of transition to intrinsic conductivity is high the higher ΔE_0 . For a given semiconductor the transition temperature is higher the higher in its impurity concentration.

Taking the relation R versus $1/T$ as the temperature decreases (cooling down to room temperature) for the same films, the results are shown in figure (5.7). It can be noticed that, the relation is irreversible Figure (5.6 & 5.7), i.e. R increases with decreasing the temperature in

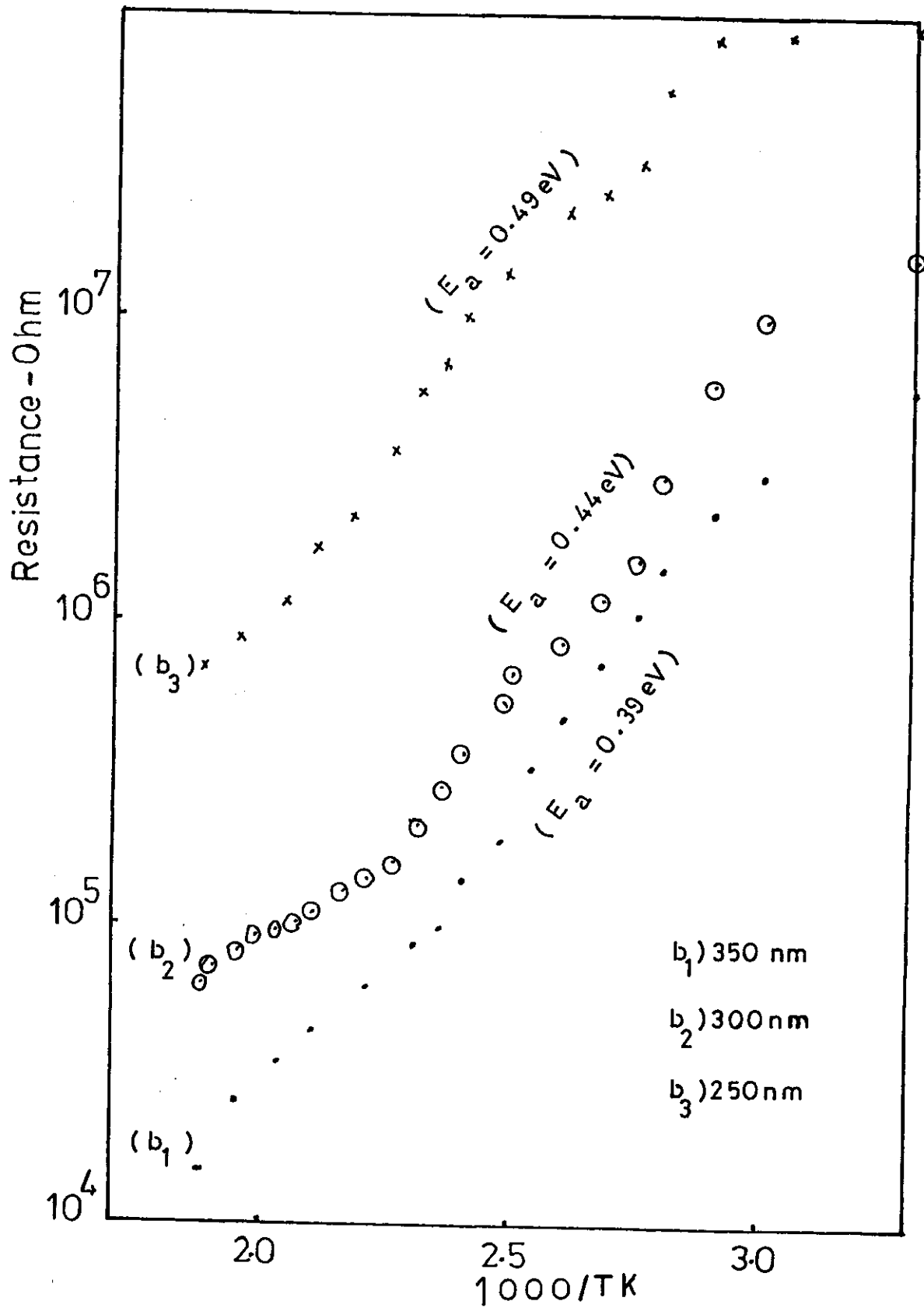


Figure (5.7)

all region from 573 K down to room temperature with one mechanism. The activation energy calculated from the linear relation of ρ , R versus $1/T$ gives ($E_a \sim 0.4-0.5$ eV) Table (5.5). Which attributed to the presence of deep donor level due to Cu, In interstitials or vacancies of S. It is also noticed that the intrinsic region not reached up to 573 K, or the energy gap due to intrinsic could not be calculated. It is attributed that the increase of defect concentration resulted from heating, increases the depletion temperature. Where after this temperature, intrinsic conductivity is controlled and the transition from band-band gives the energy gap of the semiconductor.

TABLE (5.5)

Film thickness (nm)	One region	
	TK	activation energy (eV)
$b_1 - 350$	300 - 600	0.39
$b_2 - 200$	300 - 600	0.44
$b_3 - 250$	300 - 600	0.49

The heat-treatment of CuInS_2 films of the same thickness at different temperatures before d.c. measurements are also shown. Figure (5.8) shows ρ , R versus $1/T$ for films pre-annealed at . a) 523 K, b) 573 K and 673 K in the presence of sulfur gas pressure. It can be noticed that, increasing the temperature, the resistance decreases in all cycle up to 573 K with one mechanism. The activation energy ($E_a \sim 0.14 - 0.26$ eV) due to acceptor level (sulfur interstitial). Also, there is no difference between heating and cooling cycle of measurements, Table (5.6).

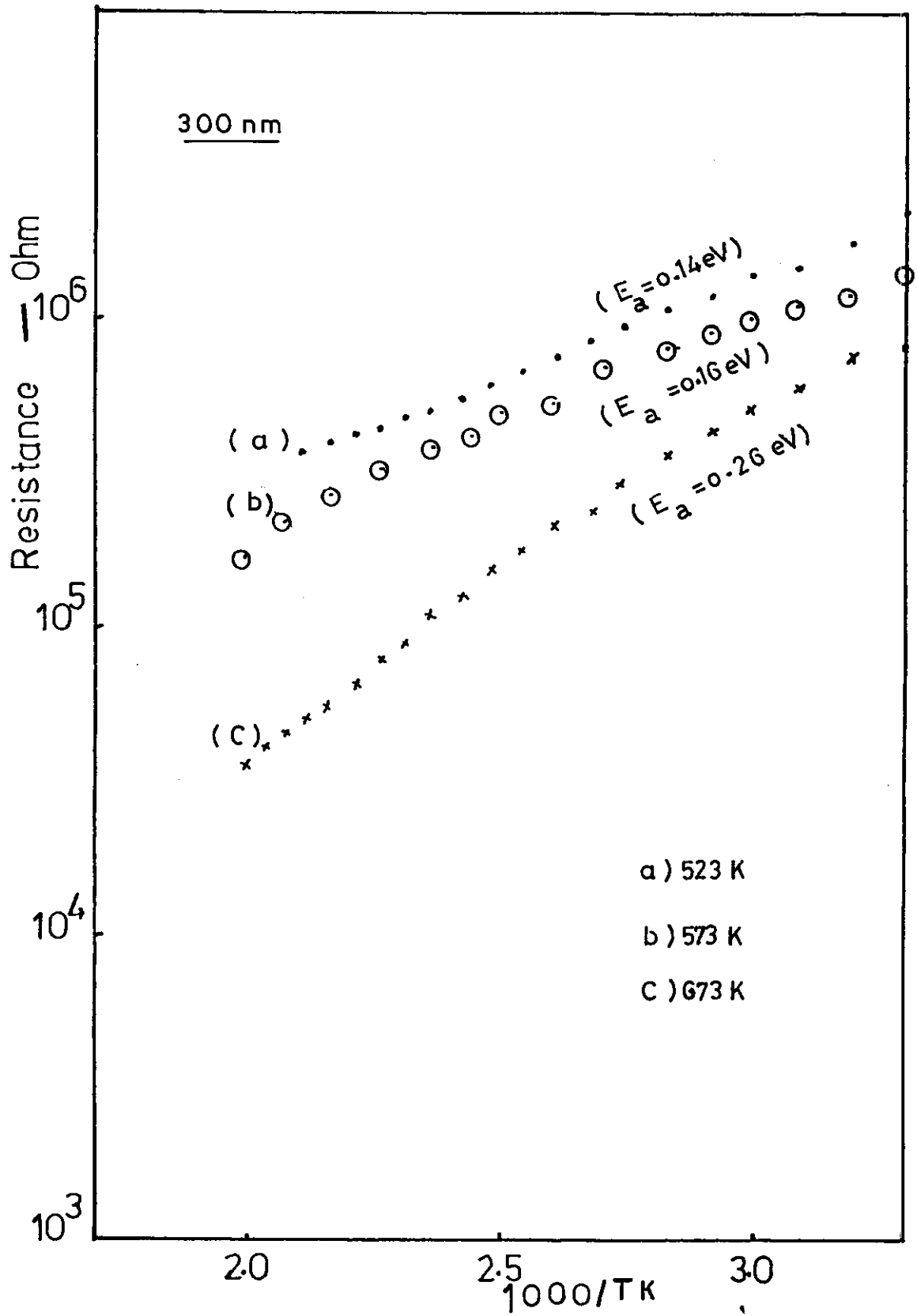


Figure (5. 8)

TABLE (5 .6)

Annealing Temperature TK	One region	
	TK	activation energy (eV)
a - 523	300 - 600	0.14
b - 573	300 - 600	0.165
c - 673	300 - 600	0.265

The resistance was reduced by heating in sulfur relative to the heating without sulfur films at room temperature figure (5.9), due to introducing excess sulfur which acts as acceptor (holes). The activation energy observed in films heat-treated was reminiscent of the acceptor level. The disappearance of the intrinsic region is observed before (92,135) and a single intense band with its principle maxima at about 0.6 eV and two distinct secondary maxima at about 0.58 eV and 0.55 eV for heat-treatment in a dynamic vacuum.

In general, the decrease in resistance after heat-treatment of the films is attributed to the presence of inclusions in the deposits as shown in scanning electron microscopy. This inclusions is mainly responsible for the large difference in the behaviour of deposit on heat treated. The formation of gaseous decomposition products from inclusions leads to detrimental effect on properties. Decomposition of inclusions may be responsible for rapid decrease of resistance with heat treatment.

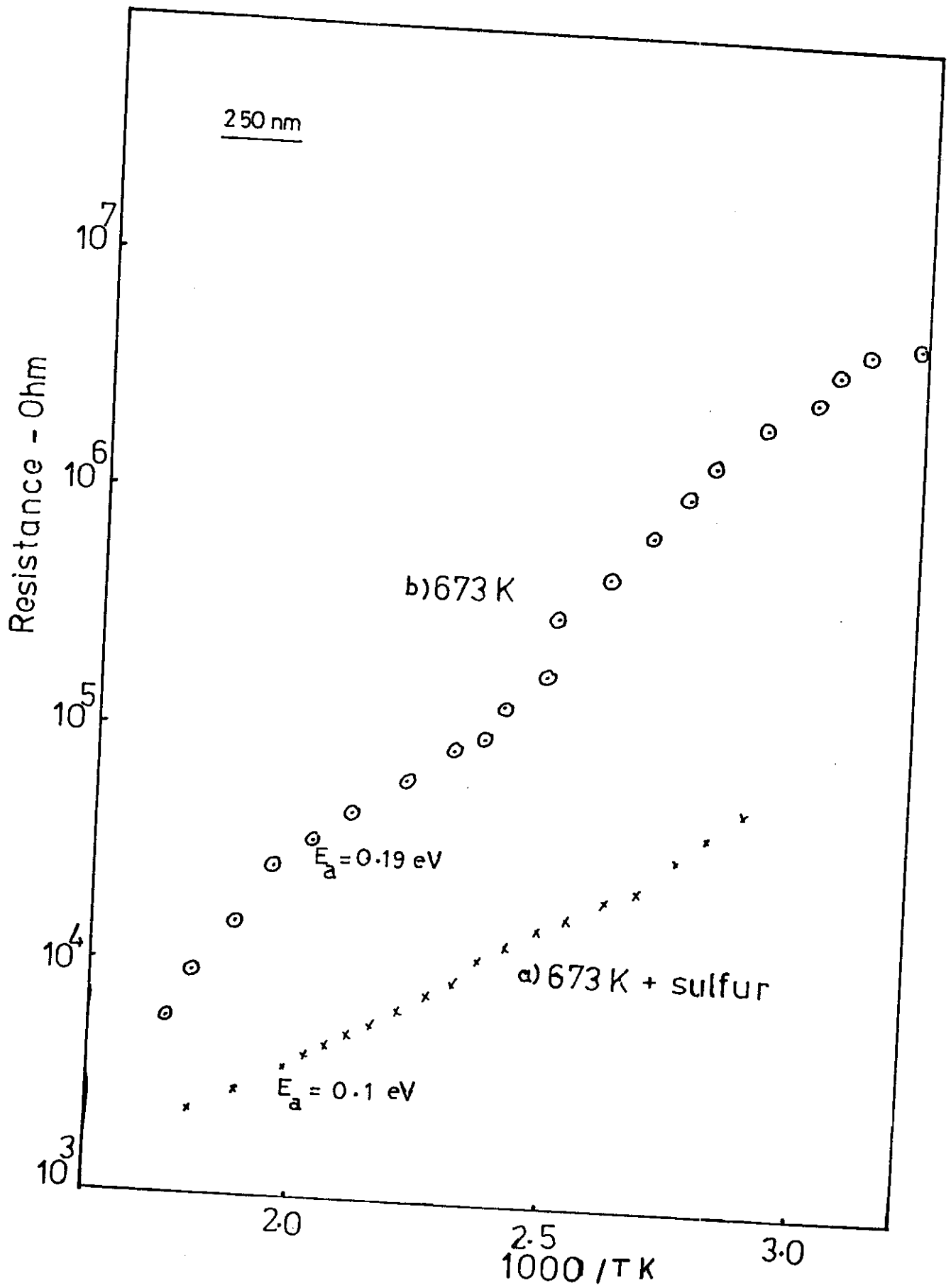


Figure (5.9)

5. B) A.C. Measurements

The impedance of chalcopyrite CuInS_2 films was measured for determining an appropriate equivalent circuit of the system. Also, the values of the circuit parameters can be estimated as; the intergranular resistance R_g , (bulk) and capacitance, C_g ; the grain boundary resistance, R_{gb} , and capacitance, C_{gb} ; besides, σ , τ_σ and ϵ .

The four basic parameters which can be obtained from the a.c. measurements are, the complex impedance, Z^* ; the admittance, Y^* ; the permittivity, ϵ^* and the modulus M^* , they are related by (122):

$$Y^* = (Z^*)^{-1} = J\omega C_0 (M^*)^{-1} = J\omega C_0 \epsilon^* \quad (5.8)$$

where, C_0 is the vacuum capacitance of the cell; $\omega = 2\pi f$ and f , is the frequency of the used bridge.

The a.c.-impedance and modulus formalisms could be used to obtain a valuable insight into the electrical properties of the samples. For a single parallel RC element, these relations may be written in the form,

$$Z^* = Z' + jZ'' \quad (5.9)$$

$$\text{where, } Z' = R / [1 + (\omega RC)^2] \quad (5.10)$$

$$, Z'' = R^2 \omega C / [1 + (\omega RC)^2] \quad (5.11)$$

$$\text{and } M^* = M' + jM'' \quad (5.12)$$

$$\text{where } M' = (\epsilon_0/C) (\omega \tau_\sigma)^2 / [1 + (\omega \tau_\sigma)^2] \quad (5.13)$$

$$\text{and, } M'' = (\epsilon_0/C) (\omega \tau_\sigma) / [1 + (\omega \tau_\sigma)^2] \quad (5.14)$$

The principle of the impedance analysis method is based on measurements of the sample impedance taken over a wide range of frequencies and then analysed in the complex impedance plane. First, consider a parallel combination of RC circuit as shown in figure (5.10.a). The impedance for such circuit at frequency, f , consists of the real part R and the imaginary part, $\frac{1}{wC}$ where $w = 2\pi f$, and is written as :

$$\frac{1}{Z} = \frac{1}{R} + jwC \quad (5.15)$$

The value of Z^* can put in the form

$$Z = R \left(\frac{1 - jw\tau}{1 + w^2\tau^2} \right) \quad (5.16)$$

where :

$$\tau = RC$$

which can be separated into the real part Z' and the imaginary part Z'' as .

$$Z' = \frac{R}{1 + w^2\tau^2} \quad (5.17)$$

and

$$Z'' = \frac{Rw\tau}{1 + w^2\tau^2} \quad (5.18)$$

by eliminating $w\tau$, these two equations (5.17), (5.18) can be combined and written in the form of a semicircle equation as :

$$Z'^2 - Z'R + Z''^2 = 0 \quad (5.19)$$

which can be written in the form:

$$(Z' - 1/2 R)^2 + Z''^2 = (1/2R)^2 \quad (5.20)$$

Comparing this equation with the standard equation of a circle, one can see that the Z^* plane plot is semicircle in the first quadrant with center at

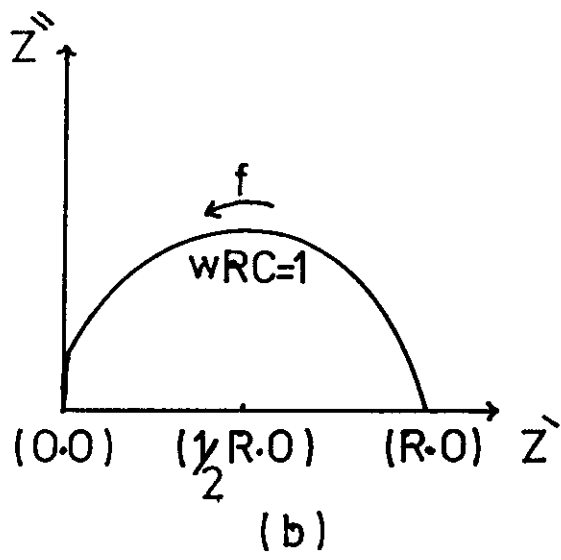
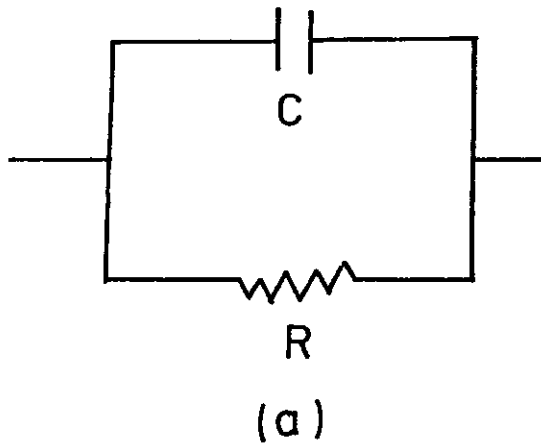


Figure (5.10)

($1/2 R$, O) and a radius $1/2 R$, as shown in figure (5.10.b). It can be shown also, that at the maximum of the semicircle, $\omega\tau = 1$, where $\tau = RC$, is the time constant or the relaxation time of the circuit. In the case of RC couple, the conductance σ , and the permittivity, ϵ' are independent of frequency thus:

$$\sigma = k / R_p \quad (5.21)$$

and

$$\epsilon' = k C_p / \epsilon_0 \quad (5.22)$$

this parallel RC element are characterized by a single Maxwell time constant, τ_σ given by :

$$\begin{aligned} \tau_\sigma &= R_p C_p \quad (5.23) \\ &= \epsilon_0 \epsilon' / \sigma \end{aligned}$$

In the light of these information the complex impedance of the CuInS_2 films was measured, at first , for various thicknesses and at different temperatures in the frequency range from 5 HZ-500 KHZ. The experimental set up for measurements was explained in details in section (2.5). The CuInS_2 films prepared by the thermal evaporation and chemical bath deposition were studied. Silver paste electrodes were employed for contacts, which show ohmic contacts. The modulus of the impedance, $|Z^*|$, was taken versus frequency for different thicknesses. As mentioned before, it was analysed to a real part, $Z' = |Z^*| \cos \theta$; and imaginary part , $Z'' = |Z^*| \sin \theta$. The real component is plotted versus frequency for thermally

prepared thick thickness film as shown in figure (5.11) and for thin thickness film as shown in figure (5.14a), also the chemically deposited films are shown in figure (5.14.b). It can be noticed that, for thick thickness thermally deposited films figure (5.11), the real part, Z' , decreases with increasing frequency reaching to a nearly constant values which differ with film thickness. This means the existence of a residual resistance connected in series with RC couple and a proposed equivalent circuit may be extracted as shown in figure (5.12). Such films condense with a discontinuous structure composed of separated grains or islands. The grains has a resistance, R_g , and capacitance, C_g , (dielectric polarization of grains) and the distances between grains has a resistance R_{gb} , and capacitance, C_{gb} (charge polarization at grain boundary). As the thickness increases the grains or islands enlarged, so, C_g vanishes and R_g remain in series with ($R_{gb} : C_{gb}$) couple. Accordingly the intergrains or interislands separation must role the mechanism of electrical conduction through the film. The charge carriers must obey certain mechanism in which the grain boundaries must act as a potential barrier of varying strength.

As going to evaluate R_g , C_g , R_{gb} and C_{gb} , the real part Z' (for thick thickness) is plotted versus Z'' , figure (5.13). It can be noticed that semicircles or arcs are obtained. Extrapolating the semicircles to meet Z' axis the values of R_g and R_{gb} can be extracted as shown. From this figures; 1) the semicircles are shifted from the origin towards the positive direction of Z' . According to the models (5.12), it means that, residual resistance in series with RC couple should be introduced. This resistance attributed to, R_g , which decreases as the thickness of the film increases tends to a constant

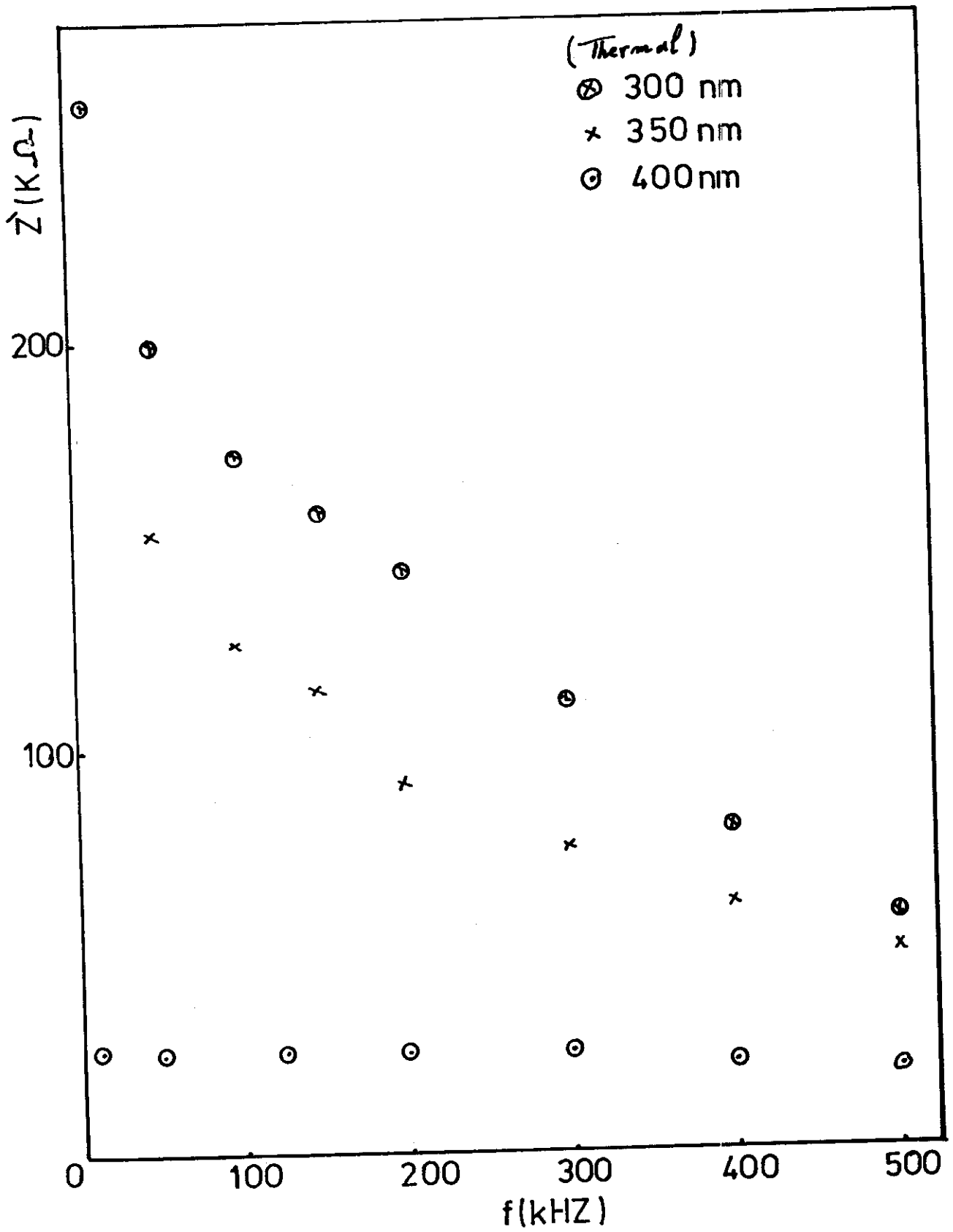


Figure (5.11)

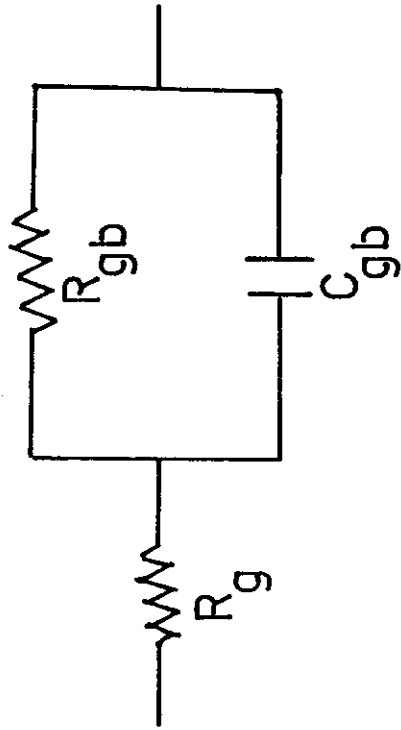


Figure (5.12)

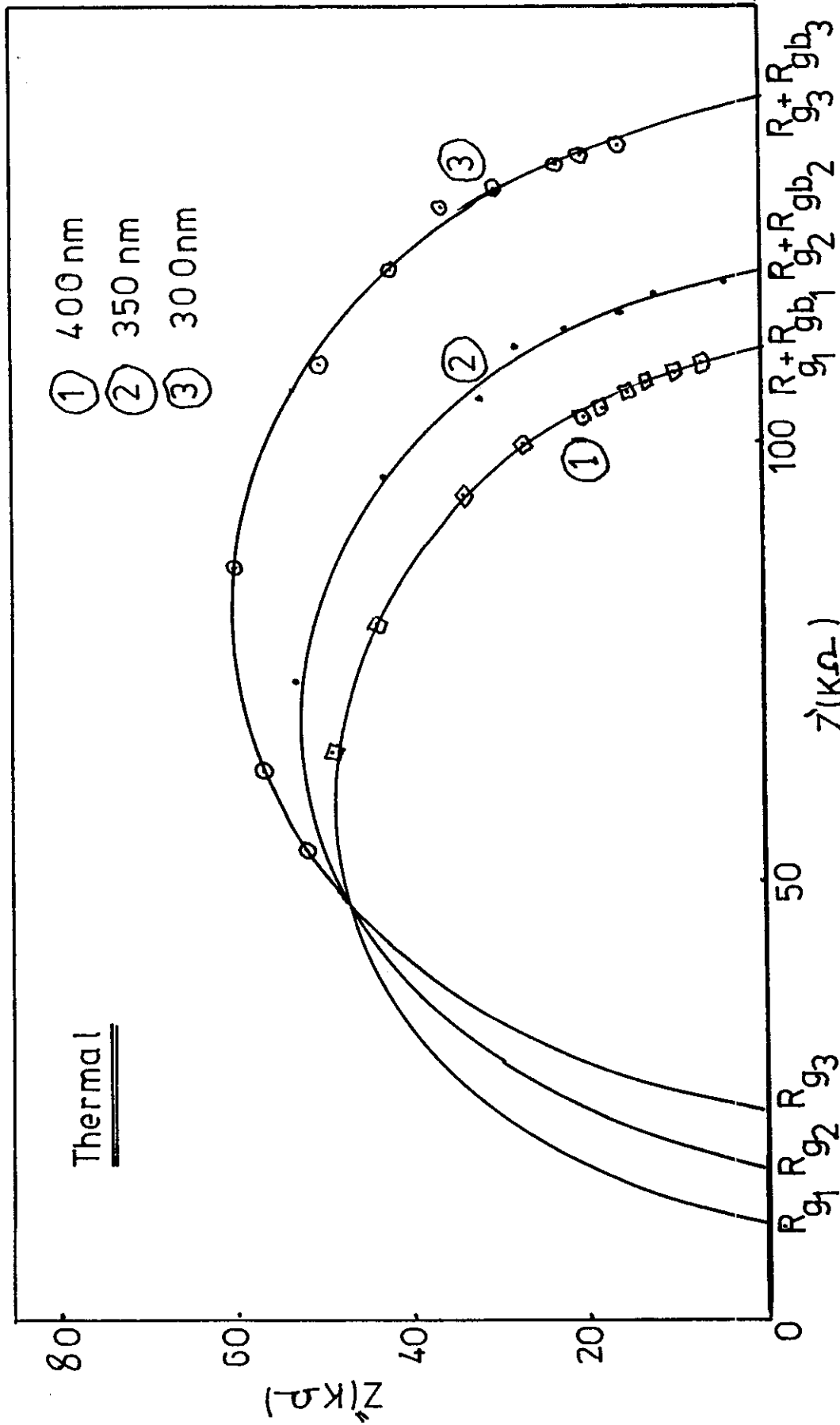


Figure (5.13)

value of the bulk resistance . 2) The far end of the semicircle meets Z'' at a value given by $R_g + R_{gb}$ which is equal to $R_{d.c}$. The values of these effects can be ascribed to stray capacity C_{gb} which shorted the R_{gb} at high frequency, where C_{gb} increases as the grain separation decreases.

In comparison, for thin thickness, the real part of impedance, Z' , is plotted versus frequency, f , figure (5.14). It can be noticed that, Z' decreases with increasing frequency more pronounced than thick films. The origin of this effect was illustrated in the equivalent circuit, corresponding to the model (5.15). Also, as the thickness decreases, the grain size decreases and the mean free path become greater than the grain diameter, so, the effect of C_g is appeared. This behaviour was noticed for thin thickness of thermally deposited and all chemically prepared films, figure (5.14.a,b). The scanning electron microscopy of these films revealed this feature, plate (3.1), (3.3), and show the existence of fine grains related to the mentioned conditions.

To calculate R_g , C_g , R_{gb} and C_{gb} , the real part Z' of these films were plotted against Z'' . As shown in figure (5.16), a semicircles were obtained, extrapolating the semicircle to meet Z' axis, the following points were noticed;

- 1) semicircles start from the origin, i.e. no residual resistance in series, and RC-couples were found.
- 2) The end of semicircles give R_g .
- 3) R_{gb} can be obtained by the knowledge of $R_{d.c}$ and $R_{gb} = R_{d.c} - R_g$
- 4) R_g and R_{gb} increases with decreasing the film thickness.

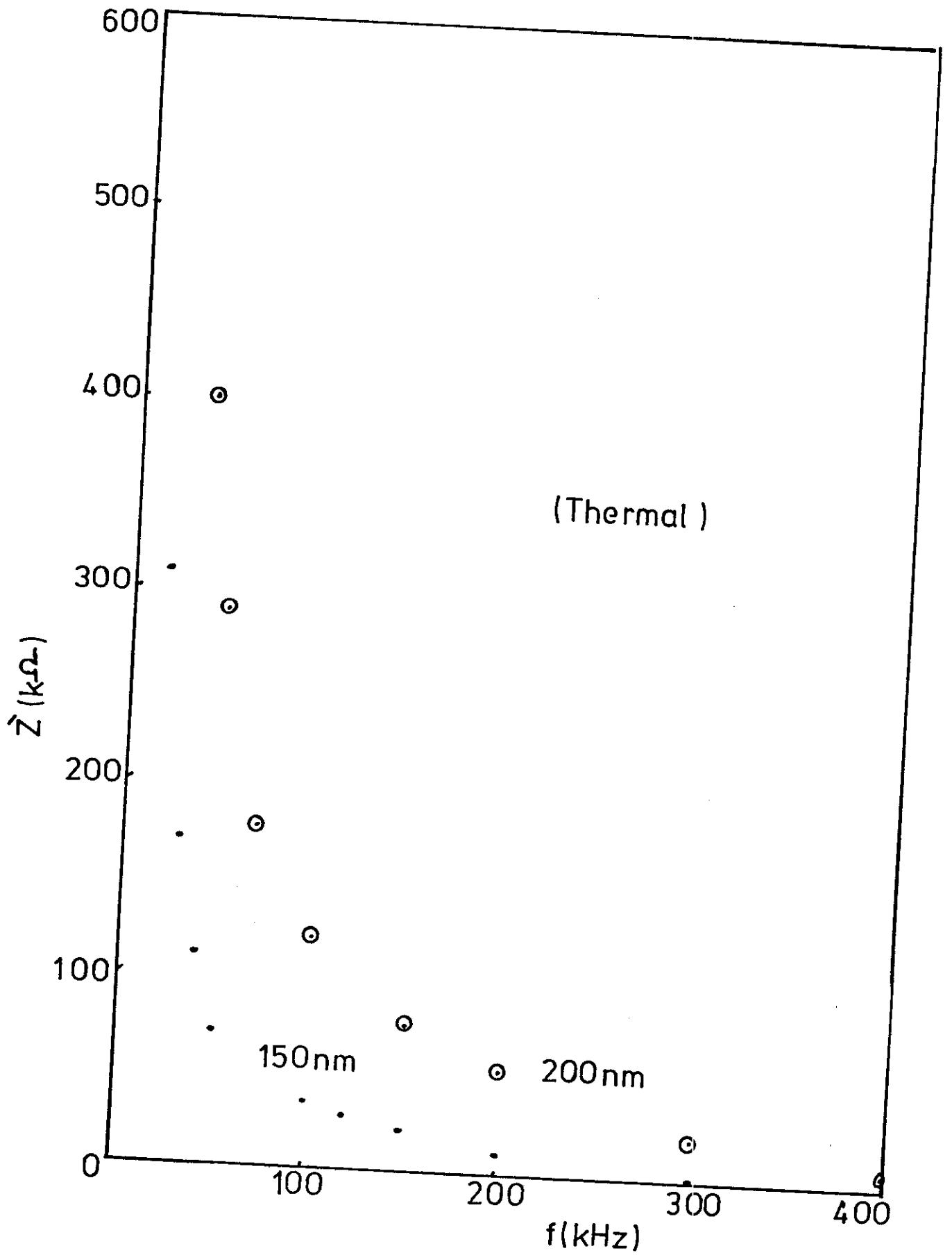


Figure (5 - 14a)

Figure (5.14 b)

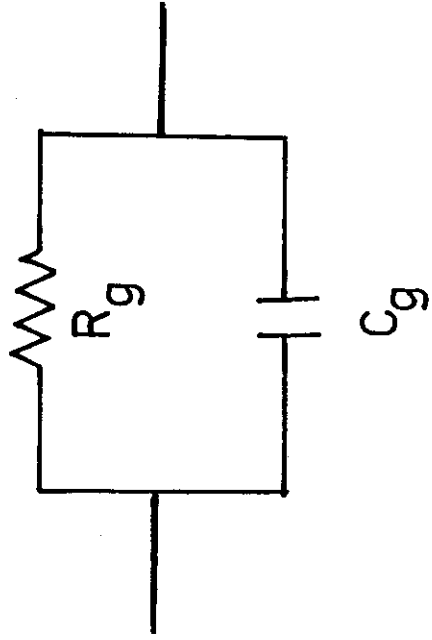


Figure (5.15)

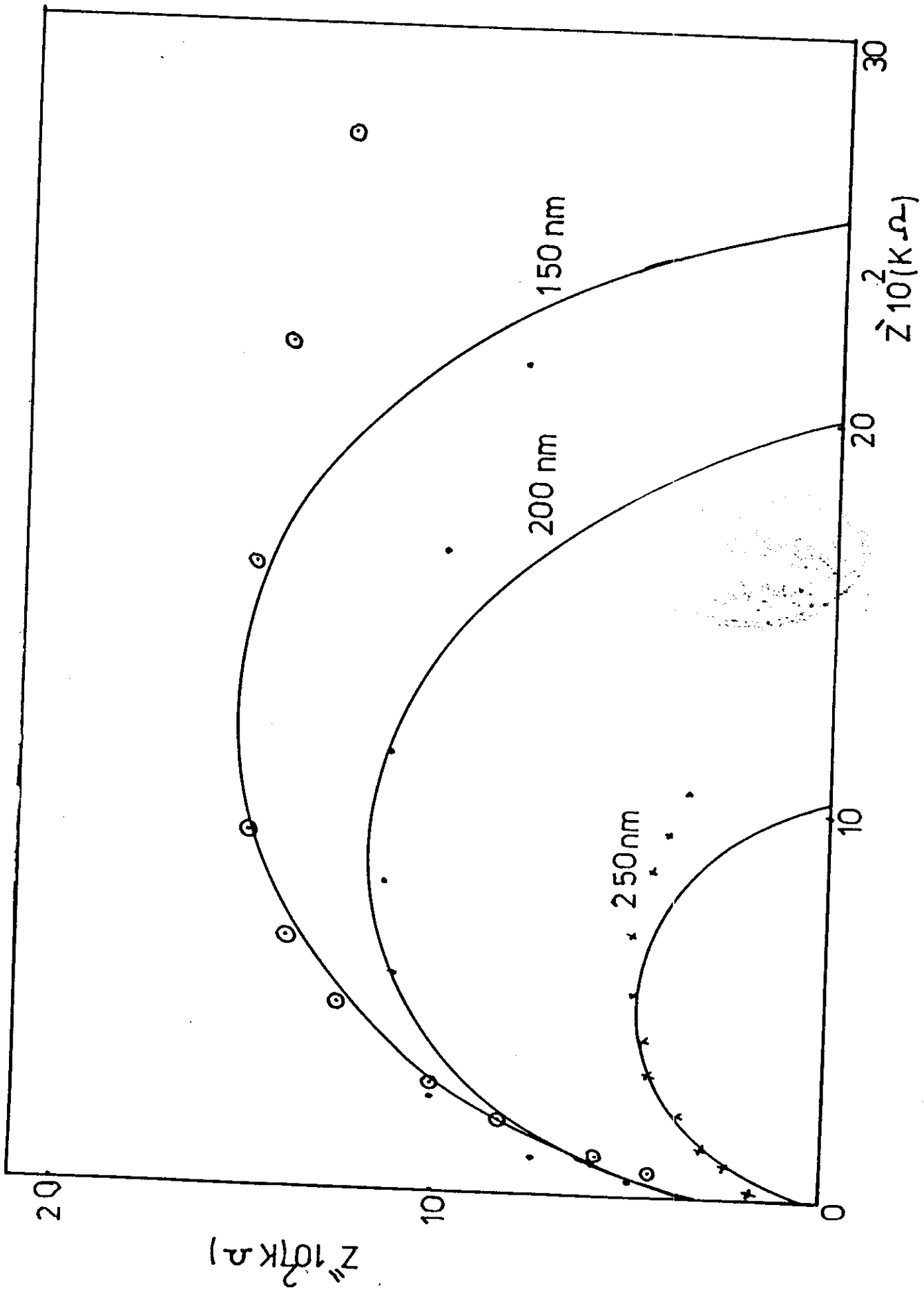


Figure (5.16)

The variation of complex impedance with temperature was also studied. Figure (5.17) shows Z' versus Z'' for different temperatures. Semicircles or arcs are obtained, the radius decreases with increasing temperature i.e. Z' or R_g and R_{gb} decrease as known of semiconductors. In general, these variations attributed to the growth of the thin film.

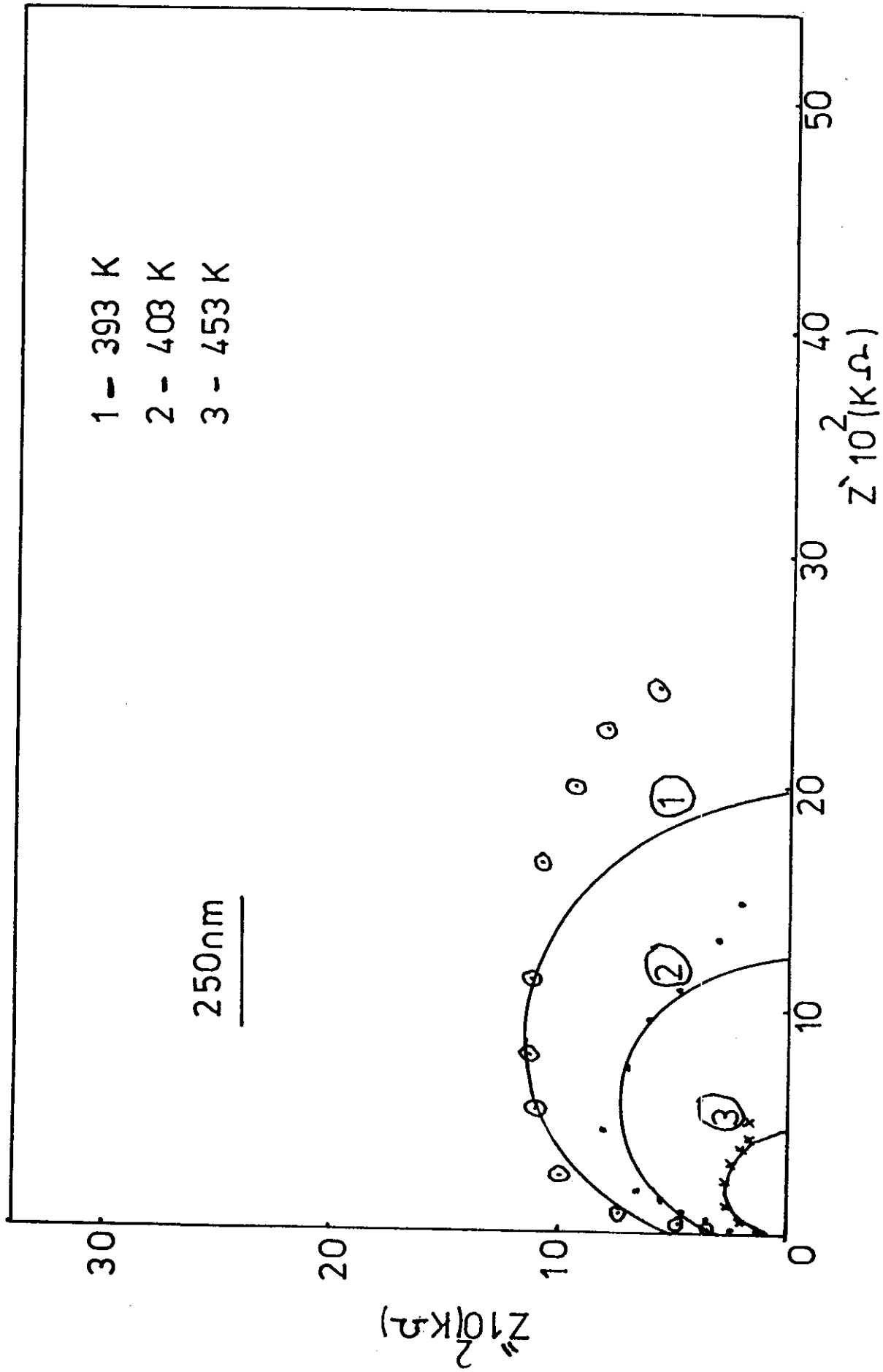


Figure (5-17)